Microstructure and properties of high-conductivity, super-high-strength Cu–8.0Ni–1.8Si–0.6Sn–0.15Mg alloy

Z. Li[a)]
School of Materials Science and Engineering, Central South University, Changsha 410083, China; and Key Laboratory of Nonferrous Metal Materials Science and Engineering, Ministry of Education, Changsha 410083, China

Z.Y. Pan
School of Materials Science and Engineering, Central South University, Changsha 410083, China

Y.Y. Zhao
Department of Engineering, University of Liverpool, Liverpool L69 3GH, United Kingdom

Z. Xiao and M.P. Wang
School of Materials Science and Engineering, Central South University, Changsha 410083, China

(Received 6 September 2008; accepted 10 February 2009)

A high-conductivity and super-high-strength alloy, Cu-8.0Ni-1.8Si-0.6Sn-0.15Mg, has been developed. The processing conditions of the alloy have been investigated. The evolution of microstructure of the alloy on aging has been examined by transmission electron microscopy. The processing condition giving the highest hardness and good electrical conductivity is as follows: solution treatment at 970 °C for 4 h, cold rolling to 60% reduction, and aging at 500 °C for 30 min. The processed alloy has an average tensile strength of 1180 MPa, 0.2% proof strength of 795 MPa, elongation of 2.75%, and average electrical conductivity of 26.5% International Annealed Copper Standard (IACS). Orthorhombic Ni_2Si precipitates are responsible for the age-hardening effect. The orientation relationship between the precipitates and the matrix is $(110)_m//(211)_p$ and $[001]_m//[01\bar{1}]_p$. DO_{22} ordering together with spinodal decomposition also contributed to the hardening.

I. INTRODUCTION

Materials for electrical applications such as connectors are required to have high strength and good electrical conductivity. Copper-matrix alloys are widely used for these applications because of their high electrical conductivity and high strength. The main copper alloy systems whose tensile strength exceeds 1000 MPa are Cu–Be, Cu–Ni–Sn, and Cu–Ti.[1–6] Cu–Ni–Sn and Cu-Ti alloys have been developed as substitutes for toxic Cu-Be alloys. However, their electrical conductivity is typically <17% IACS, which is much lower than that of Cu–Be alloys [the electrical conductivity of QBe2, for example, has a typical value of 25% International Annealed Copper Standard (IACS)]. There is a need to develop new alloys with better combinations of strength and electrical conductivity.

Cu–Ni–Si-based alloys have created considerable interest because they have both high strength and high electrical conductivity.[7–9] The high strength in these alloys is caused by the large quantity of nanoscale precipitates formed during aging. These precipitates increase the strength of the alloy markedly, without significant sacrifice of electrical conductivity.[10–13] Mg and Sn additions can produce higher strength and resistance to stress relaxation.[14] The improvement of strength or stress relaxation resistance is caused by the decrease in interprecipitate spacing by the Mg addition or by the Mg-atom-drag effect on dislocation motion.[14] As a consequence, Cu–Ni–Si-based nanoscale dispersion-strengthened alloys with high solute concentrations have a good prospect for replacing Cu–Be alloys in many applications. However, there is limited study in the development of this alloy system. Until now, no alloys in this system have been reported to have a tensile strength higher than 1100 MPa.

This paper reports on the development of a Cu–8.0Ni–1.8Si–0.6Sn–0.15Mg (wt%) alloy, which has a high tensile strength of 1180 MPa and a high electrical conductivity of 26.5% IACS. The procedure of preparation, the thermo-mechanical treatment, and the resultant microstructure and properties are investigated.

II. EXPERIMENTAL PROCEDURES

A Cu–Ni–Si–Sn–Mg alloy ingot was prepared using a medium-frequency induction furnace. Prespecified quantities of Cu, Ni, and Sn blocks were first melted

[a)]Address all correspondence to this author.
e-mail: lizhou6931@163.com
DOI: 10.1557/JMR.2009.0251

in the furnace. Intermetallic Cu–Mg and Cu–Si master alloys of the required quantities were added to the molten bath, producing a chemical composition of Cu–8.0Ni–1.8Si–0.6Sn–0.15Mg. The melting and casting operations were carried out in a N_2 atmosphere to prevent the alloy from oxidizing. After surface defects were removed, the ingot was homogenized at 930 °C for 24 h and subsequently rolled at 900 °C, reducing the ingot thickness from 20 to 4 mm. The resultant strip was solution-treated at different temperatures of 950, 970, or

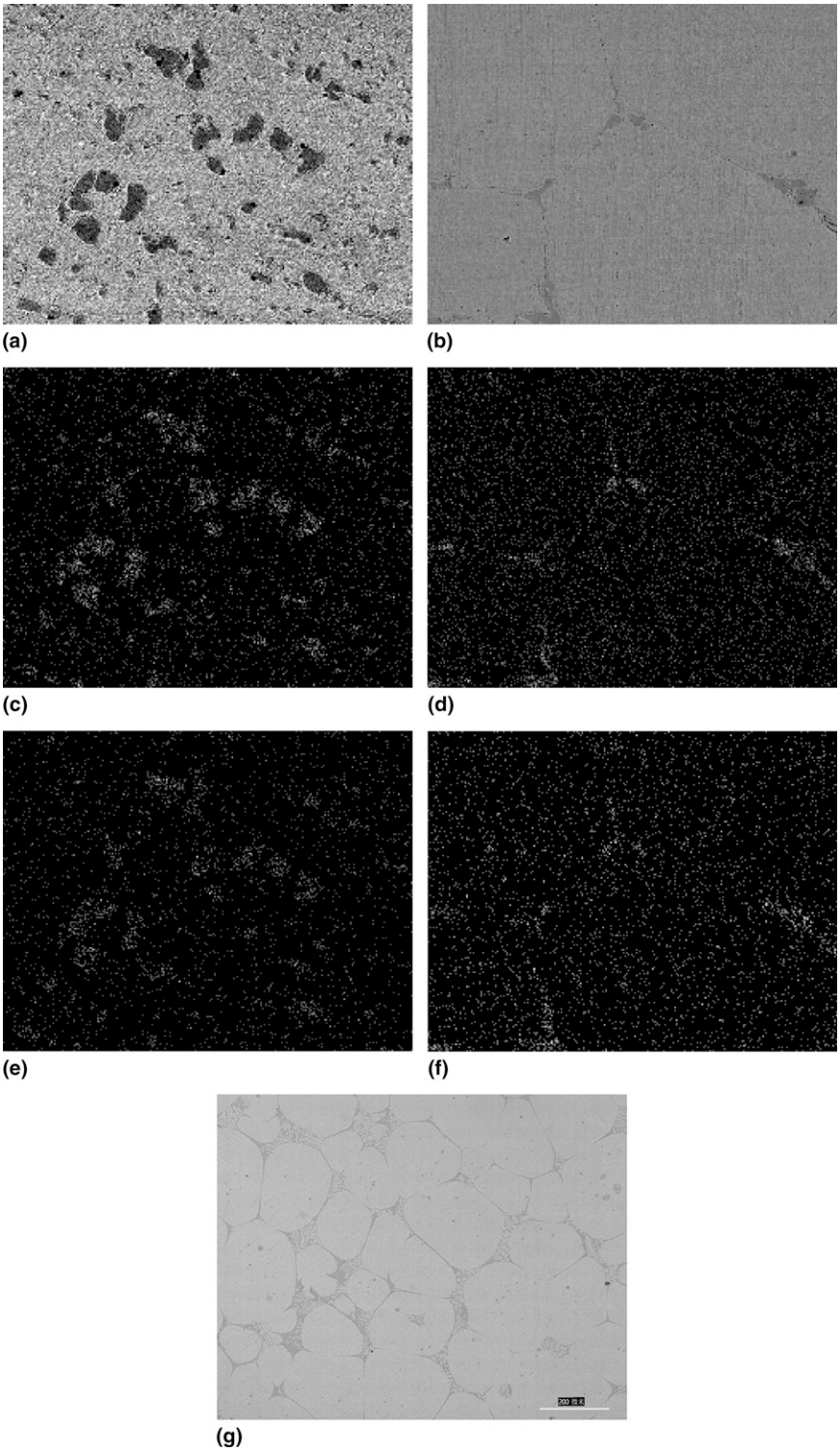

FIG. 1. SEM micrograph and the elemental mapping images of the alloy solution treated at 950 °C, 970 °C, and 980 °C for 4 h, respectively.

980 °C for 4 h in a N_2 + H_2 atmosphere, followed by water quenching. It was subsequently cold rolled with a 60% reduction in thickness, aged at 500 °C in a salt bath for various periods of time, and water-cooled to room temperature. A series of samples were taken at different stages of the solution and aging treatment for microstructural and mechanical analysis.

The microhardness of the samples was measured on a HV-5 Vickers hardness machine (Laizhou Huayin Testing Instrument Co., Shandong, China) using a load of 3 Kgf and a holding time of 15 s. Tensile tests of the samples were conducted on an Instron 8019 tester. The microstructure of the samples at different heat treatment stages was observed using scanning electron microscope (SEM) Sirion 200 (Instron Corp., Norwood, MA) and transmission electron microscope (TEM) H-800 (Hitachi, Tokyo, Japan) with an operation voltage of 200 KV.

III. RESULTS AND DISCUSSION

A. Solution treatment temperature

Figure 1 shows typical SEM micrographs and the Ni and Si elemental mapping images of the samples solution-treated at 950, 970, and 980 °C. At 950 °C, a large number of large particles are clearly visible [Fig. 1(a)]. The elemental mapping images taken from Fig. 1(a) are shown in Figs. 1(c) and 1(e), which indicate that the particles are rich with Ni and Si. This solution temperature is apparently not high enough to dissolve the alloying elements into a solid solution, and, as a consequence, considerable amounts of the alloying elements exist in the form of dispersoids formed in the previous casting. At 970 °C, only a small number of second-phase particles exist at the grain boundaries [Fig. 1(b)]. Again, these particles are rich with Ni and Si [Figs. 1(d) and 1(f)]. Apart from these dispersoids at the boundaries, however, Ni and Si distribute uniformly within the grains. At 980 °C, a eutectic phase manifests nearly continuously at the grain boundaries [Fig. 1(g)], which can lead to significant decrease in the mechanical properties. Overall, the optimum solution treatment temperature is 970 °C, at which most dispersoids are dissolved in the solid solution and the eutectic phase is not formed. All the samples for further studies were solution treated at 970 °C in this study.

B. Properties

The microhardness and electrical conductivity of the samples were measured after they were solution-treated at 970 °C for 4 h, cold rolled, and aged at 500 °C. The variations of the average microhardness and electrical conductivity as a function of aging time are shown in Figs. 2 and 3, respectively. Both the average microhardness and average electrical conductivity increase rapidly with aging time up to 30 min. The average microhardness reaches its maximum value of 345 Hv in 30 min and decreases slightly with increasing aging time. The average electrical conductivity increases only slightly with prolonging the aging time further after 30 min. The optimum aging time for the best combination of hardness and electrical conductivity is therefore 30 min.

After solution treatment at 970 °C for 4 h, cold rolling to 60% reduction, and aging at 500 °C for 30 min, the Cu–Ni–Si–Sn–Mg alloy has an average tensile strength of 1180 MPa, 0.2% proof strength of 795 MPa, elongation of 2.75%, and an average electrical conductivity of 26.5% IACS. The alloy not only has a high strength but also an electrical conductivity higher than that of QBe2, which has a typical value of 25% IACS.

C. Microstructure

Figures 4(a) and 4(b) are two typical TEM images of a sample solution treated at 970 °C for 4 h, cold rolled to 60% reduction, and aged at 500 °C for 30 min. These two images are representative for practically the entire microstructure of the alloy in the aged state. The electron-diffraction patterns of Figs. 4(a) and 4(b) are shown

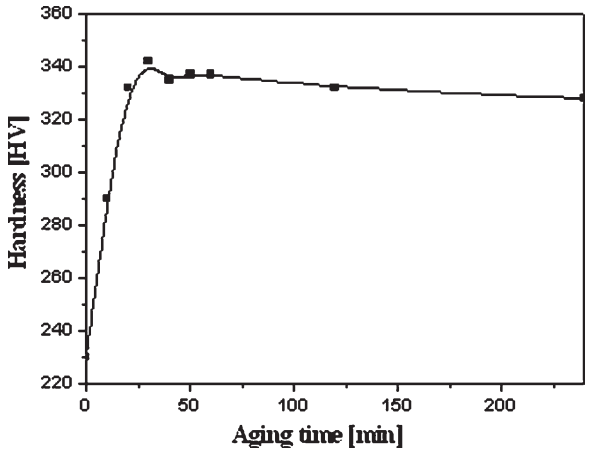

FIG. 2. Evolution of average microhardness with aging time.

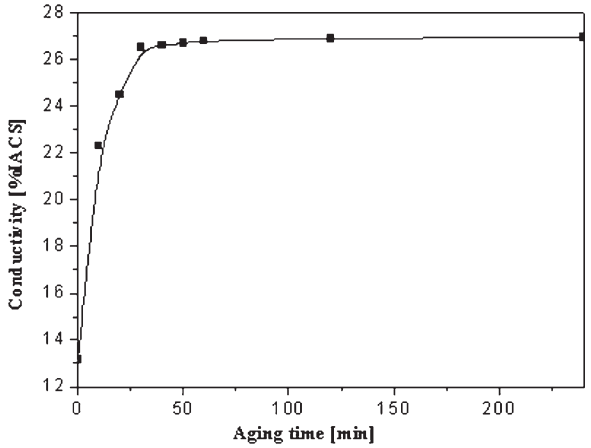

FIG. 3. Variation of average electrical conductivity with aging time.

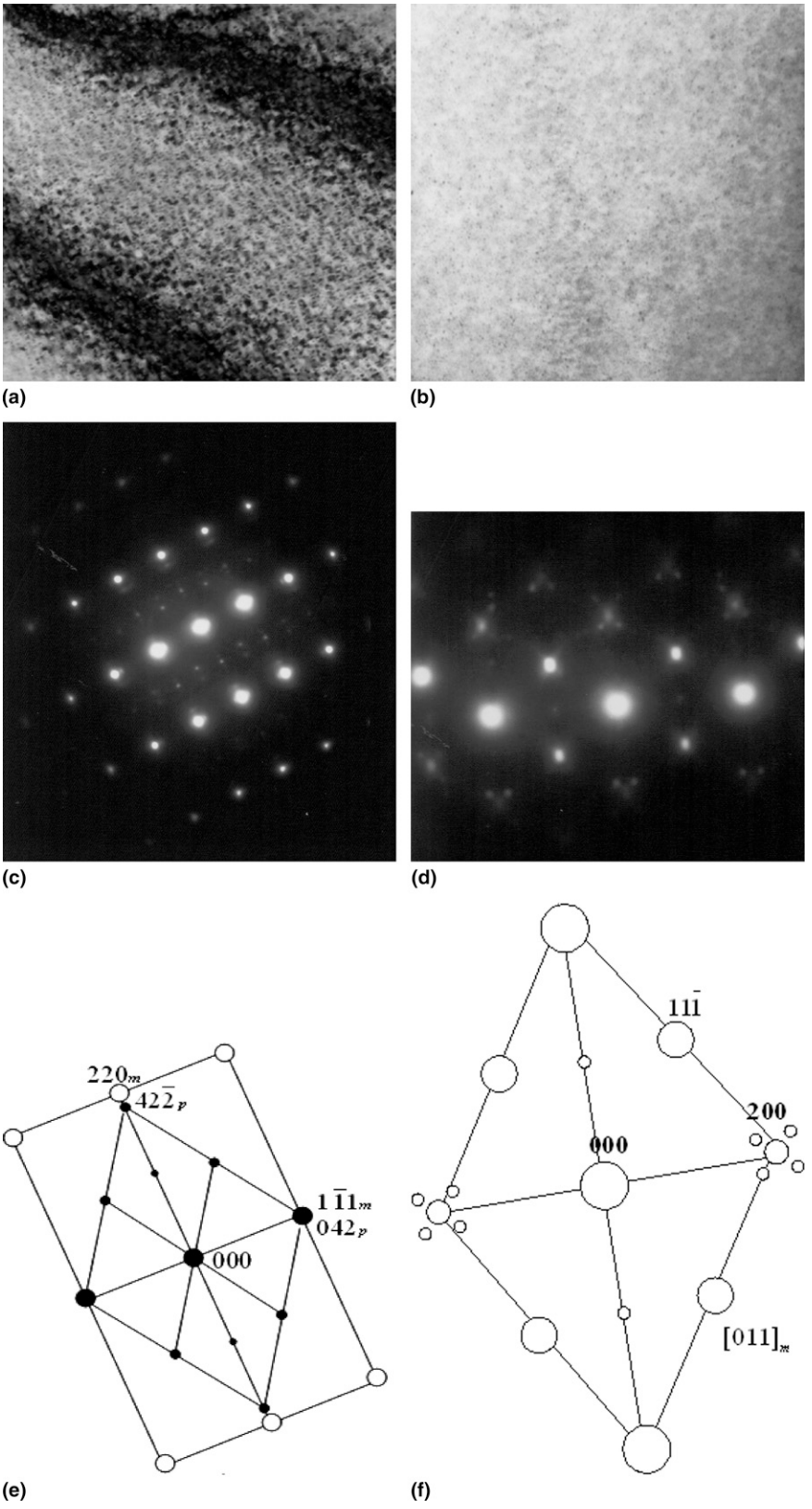

FIG. 4. (a, b) TEM images of thin foil samples aged at 500 °C for 30 min.

in Figs. 4(c) and 4(d), and their corresponding pattern analyses are shown in Figs. 4(e) and 4(f), respectively.

Figure 4(a) shows that a large amount of particles precipitated during aging, and these precipitates have a structure corresponding to orthorhombic Ni_2Si [see Fig. 4(c)]. The orientation relationship between the precipitates and the matrix is determined to be $(110)_m//(211)_p$, $[001]_m//[01\bar{1}]_p$ [see Fig. 4(e)]. The superlattice reflections from ordering can be seen in Fig. 4(c) (indicated by the arrow). The compositions of the dark banding shown in Fig. 4(a) were determined by energy-dispersive x-ray analysis (EDX) and are collected in Table I. The dark banding is Ni_2Si phase-rich layers.

TABLE I. Compositions of the dark banding determined EDX.

Element	Wt%	At.%
Si K	17.55	30.79
Ni K	82.45	69.21

Figure 4(b) shows that, in addition to the precipitation particles, there are discontinuous precipitation colonies. The satellites of modulation in the electron diffraction pattern, indicated by arrows in Fig. 4(d), show the existence of structure modulation in the sample.[11,12] The structural modulation, resulting from spinodal decomposition, is found to occur along the {001} directions. Precipitation, spinodal decomposition, and ordering all take place in this sample as it was aged at 500 °C for 30 min.

Figure 5 shows the selected area diffraction patterns (SADPs) of a sample aged at 500 °C for 30 min. The [001], [110], [012], and [111] zone diffraction patterns are shown in Figs. 5(a), 5(b), 5(c), and 5(d), respectively.

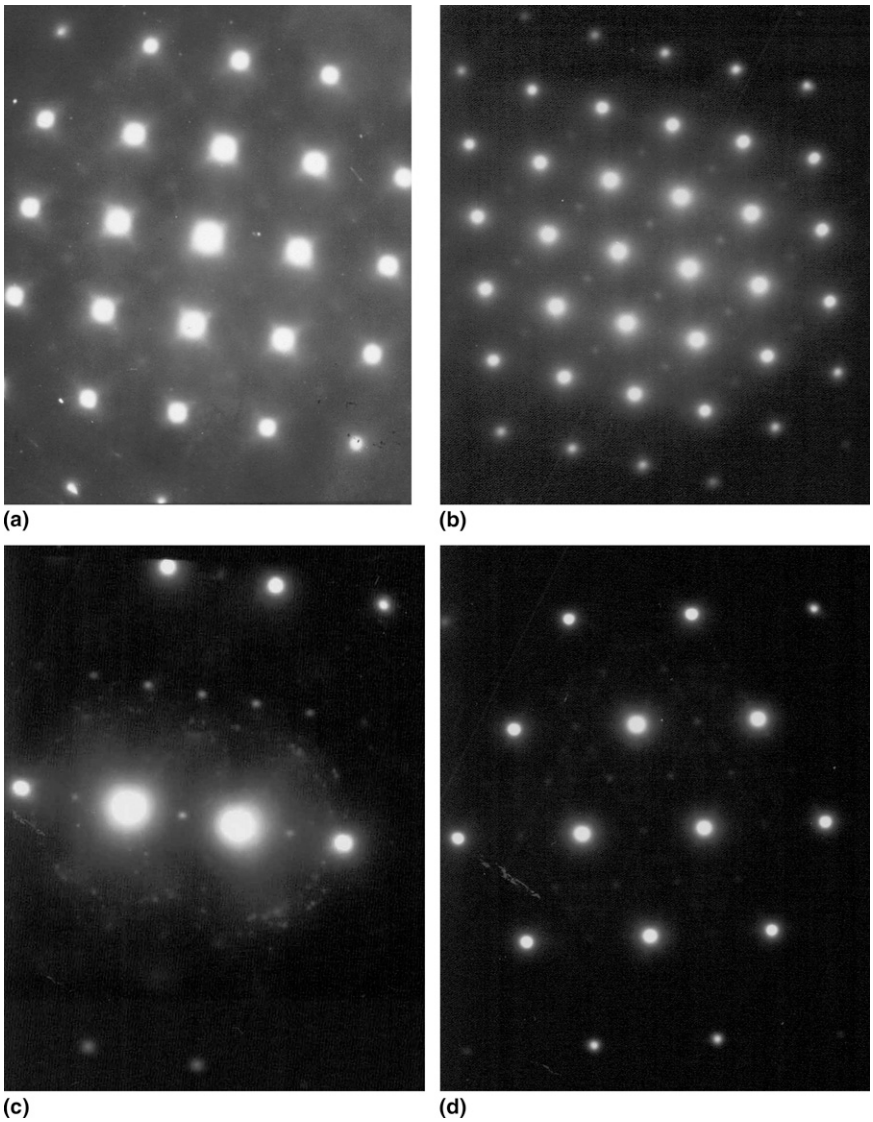

FIG. 5. The SADPs of different field of view of the alloy aged at 500 °C for 30 min.

The superlattice reflections found in Figs. 5(a) and 5(b), 5(c), and 5(d) are {011}, $\{0\frac{1}{2}1\}$, and $\{\frac{1}{2}\frac{1}{2}1\}$ types, respectively. Because the $\{0\frac{1}{2}1\}$ and $\{\frac{1}{2}\frac{1}{2}1\}$ types reflections are unique to DO_{22}, it is clear that DO_{22} ordering takes place in the alloy aged at 500 °C for 30 min. The SADPs in this experiment, however, cannot confirm the coexistence of short-range order $L1_2$ and long-range order DO_{22}, because all the $L1_2$ superlattice reflections ({001} and {011} types) overlap with some of the DO_{22} superlattice reflections.

D. Strengthening mechanism

Precipitation hardening is the dominant mechanism responsible for the high strength of the Cu–Ni–Si–Sn–Mg alloy in this study, although DO_{22} ordering[15,16] and spinodal decomposition[17,18] also contribute to the hardening. The microstructural changes in the alloy during aging are expected to be similar to the structural transition sequence in a Cu–Ni–Si alloy studied by Zhao et al.[12] However, the addition of Mg affects precipitation kinetics and increases the formation rate of Ni_2Si precipitates.[14] At the initial stage of aging, the supersaturated solid solution decomposes by the spinodal mechanism into periodic Si-rich and Si-poor regions. As the aging treatment proceeds, a metastable ordered phase with the DO_{22} [$(Cu,Ni)_3Si$] structure results. On further aging, Ni_2Si precipitates are formed.[12] When the aging time is <30 min, the amount of the precipitates is small; the hardening, or the increase of hardness, is mainly attributed to the ordering together with spinodal decomposition. The maximum microhardness achieved at an aging time of 30 min is an outcome of a great number of nanoscale Ni_2Si precipitates. The particles of Ni_2Si are difficult to shear by dislocation, and the dislocation only bypasses it. The increase of yield stress by the nanoscale Ni_2Si precipitations can be described by the Orowan mechanism; the increment $\Delta\sigma_{Orowan}$[19,20] is as follows:

$$\Delta\sigma_{\mathrm{Orowan}} = \frac{0.81MGb}{2\pi(1-\nu)^{1/2}}\frac{\ln(d_p/b)}{(\lambda - d_p)} \quad , \qquad \lambda = \frac{1}{2}d_p\sqrt{\frac{3\pi}{2f_v}} \tag{1}$$

where, M is Taylor-factor (M of Cu is 3.1); G is the shear modulus of matrix (the shear modulus of Cu is 45.5 GPa); ν is the Poisson's ratio (= 0.34); b is the Burgers vector (= 0.255 nm); and λ is the average particle plane square lattice spacing (i.e., apparent particle spacing). d_p is the average particle diameter. f_v is the volume fraction of particle.

The yield stress increases as the average particle diameter decreases. The longer the aging time, the more the hardness of alloy decreases, which is because of growing of precipitation particles that decreases the alloy's strength as shown by Eq. (1). The typical morphology of the alloy aging at 500 °C for 1 h is shown in Fig. 6; the precipitation particles course obviously compared with those in Fig. 4(a).

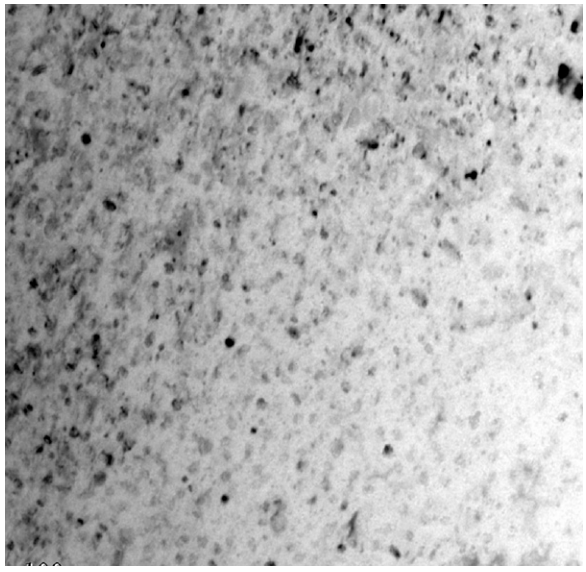

FIG. 6. The TEM BF of the alloy aging at 500 °C for 1 h.

The electrical conductivity of the alloy in the aged state is mainly dependent on the purity of the copper matrix and to a much less extent on the size and number of the precipitates. The removal of solute elements from the copper matrix by the formation of precipitates decreases scattering of electrons. The lowered strain energy between the matrix and precipitates during the aging process can also reduce the scattering to electrons. Both lead to the increase of electrical conductivity with aging time.

IV. CONCLUSIONS

A super-high-strength Cu–8.0Ni–1.8Si–0.6Sn–0.15Mg alloy has been developed. The alloy, subjected to solution treatment at 970 °C for 4 h, cold rolling to 60% reduction, and aging at 500 °C for 30 min, has an average tensile strength of 1180 MPa, 0.2% proof strength of 795 MPa, elongation of 2.75%, and an average electrical conductivity of 26.5% IACS. Orthorhombic Ni_2Si precipitates are responsible for the age-hardening effect. The orientation relationship between the precipitates and the matrix is $(110)_m//(211)_p$ and $[001]_m//[01\bar{1}]_p$. DO_{22} ordering together with spinodal decomposition also contributed to the hardening. This alloy with high conductivity and super high strength has a good prospect for replacing toxic Cu–Be alloys in many applications.

ACKNOWLEDGMENT

This work is supported by the "863" Project (2006AA03Z517) of the Ministry of Science and Technology of the People's Republic of China.

REFERENCES

1. P. Lehtinen, T. Tiainen, and L. Laakso: New continuously cast CuNiSn alloys provide excellent strength and high electrical conductivity. *Metall. (Germany)* **50**(4), 267 (1996).
2. M. Masamichi and O. Yoshikiyo: Influence of solution-treatment conditions on the cellular precipitation in Si-doped Cu-10Ni-8Sn alloy. *Mater. Trans., JIM* **32**(12), 1135 (1991).
3. H. Tsubakino, R. Nozato, and A. Yamamoto: Precipitation sequence for simultaneous continuous and discontinuous modes in Cu-Be binary alloys. *Mater. Sci. Technol.* **19**(4), 288 (1993).
4. M. Masamichi and O. Yoshikiyo: Effect of B additions on the intragranular and celluar precipitations in a Cu-Be alloy. *Mater. Trans., JIM* **29**(11), 903 (1988).
5. W.A. Soffa and D.E. Laughlin: High-strength age hardening copper–titanium alloys: Redivivus. *Prog. Mater. Sci.* **49,** 347 (2004).
6. S. Nagarjuna, K. Balasubramanian, and D.S. Sarma: Effects of cold work on precipitation hardening of Cu-4.5mass% Ti alloy. *Mater. Trans., JIM* **36,** 1058 (1995).
7. H. Fujiwara: Effect of alloy composition on precipitation behavior in Cu-Ni-Si alloys. *J. Jpn. Inst. Met.* **62**(4), 301 (1998).
8. H.J. Ryu, H.K. Baik, and S.H. Hong: Effect of thermomechanical treatments on microstructure and properties of Cu-base leadframe alloy. *J. Mater. Sci.* **35,** 3641 (2000).
9. S. Suzuki, N. Shibutani, K. Mimura, M. Isshiki, and Y. Waseda: Improvement in strength and electrical conductivity of Cu-Ni-Si alloys by aging and cold rolling. *J. Alloys Compd.* **417,** 116 (2006).
10. H. Nagayoshi, F. Nishijima, and C. Watanabe: Bend formability and microstructure in a Cu-4 mass%Ni-1 mass%Si-0.02 mass%P alloy. *J. Jpn. Inst. Met.* **70**(9), 750 (2006).
11. R. Monzen and C. Watanabe: Microstructure and mechanical properties of Cu-Ni-Si alloys. *Mater. Sci. Eng., A* **483–484,** 117 (2008).
12. D.M. Zhao, Q.M. Dong, and P. Liu: Structure and strength of the age hardened Cu–Ni–Si alloy. *Mater. Chem. Phys.* **79,** 81 (2003).
13. S. Suzuki, N. Shibutani, K. Mimura, M. Isshiki, and Y. Waseda: Improvement in strength and electrical conductivity of Cu-Ni-Si alloys by aging and cold rolling. *J. Alloys Compd.* **417,** 116 (2006).
14. R. Monzen, C. Watanabe, Z.G. Zhang, and R. Monzen: Microstructure and mechanical properties of Cu-Ni-Si alloys. *J. Soc. Mat. Sci. Jpn.* **54,** 717 (2005).
15. J.C. Zhao and M.R. Notis: Spinodal decomposition, ordering transformation, and discontinuous precipitation in a Cu-15Ni-Sn alloy. *Acta Mater.* **46**(12), 4203 (1998).
16. Ph. Goudeau, A. Naudon, and J.M. Welter: Anomalous small-angle x-ray scattering study of the early stages of decomposition in Cu-15wt%Ni-8wt%Sn. *J. Appl. Crystallogr.* **266,** 23 (1990).
17. E. William: Hardening during the late stages of spinodal decomposition. *Mater. Sci. Eng.* **77,** 27 (1986).
18. S.S. Kim, J.C. Rhu, and Y.C. Jung: Aging characteristics of thermomechanically processed Cu-9Ni-6Sn alloy. *Scr. Mater.* **40** (1), 1 (1999).
19. M. Mabuchi: Strengthening mechanism of Mg-Si alloy. *Acta Mater.* **44**(11), 4611 (1996).
20. J. Lee, J.Y. Jung, E.S. Lee, W.J. Park, S. Ahn, and N.J. Kim: Microstructure and properties of titanium boride dispersed Cu alloys fabricated by spray forming. *Mater. Sci. Eng., A* **277,** 274 (2000).